Experimental Investigation of Droplet-Droplet Interactions

R. Bordás*, T. Hagemeier and D. Thévenin
Laboratory of Fluid Dynamics & Technical Flows
University of Magdeburg "Otto von Guericke"
Magdeburg, D 39106, Germany

Abstract

Shadowgraphy is an established imaging measurement method, allowing in particular to determine droplet velocity and diameter distributions. One advantage of Shadowgraphy compared to other non-intrusive measurement methods is its ability to directly observe collision and coalescence processes. As the expected collision probability in many practical two-phase flows is moderate and the acquisition frequency of the Shadowgraphy system is limited, this measurement method must be optimized for the investigation of droplet-droplet interactions. In this work it is shown that Shadowgraphy can be indeed applied to a quantitative investigation of collision events. For this purpose the software (DaVis 7.2 from LaVision) has been considerably improved with the help of its built-in macro language, allowing an automatic analysis of the measurement results. The resulting experimental procedure has been tested using measurements in a two-phase wind tunnel. Corresponding results are compared with available theoretical predictions.

Introduction

The collision rate of water droplets in a turbulent flow is a key property to understand many practical issues. It is for instance needed for numerical predictions of rain soiling or warm rain initiation in cumulus clouds, as is one objective of the MetStroem priority program (SPP 1276), founded by the DFG (German Research Foundation). Both theoretical [1] and numerical [2] investigations are available in the literature, but there is a lack of reliable experimental data for droplet-droplet interactions in turbulent flows with controlled conditions. The purpose of the present work is the development of a suitable experimental data-base, allowing model testing and improvement by comparing a posteriori theoretical predictions and measurements. In order to allow a detailed analysis, both the continuous gas phase and the dispersed liquid phase are characterized in detail, including droplet-droplet interactions. In what follows, the application of the Shadowgraphy technique to investigate experimentally collision events in a controlled turbulent flow is presented.

Experimental Setup

The central goal of these experiments is to measure the collision rate in a turbulent horizontal channel flow of air containing dispersed droplets. The particle and turbulence properties have been quantified using different optical measurement techniques. In the following, the two-phase wind tunnel is first described, the measurement configurations are characterized and the Shadowgraphy method is finally discussed.

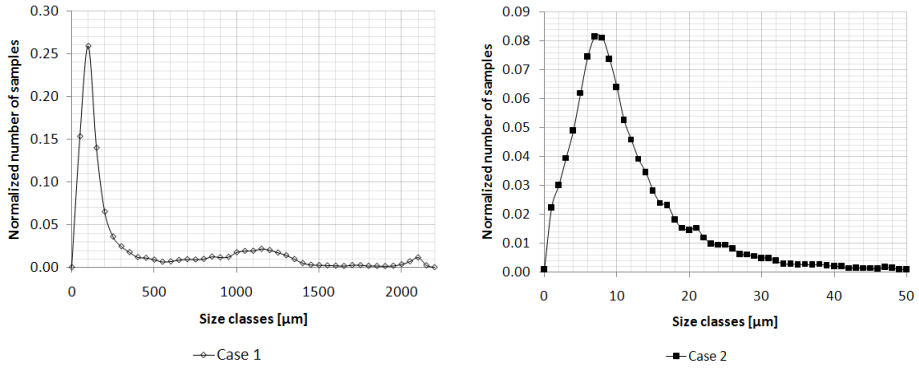

Figure 1. Size distribution for Case 1 (left) and Case 2 (right).

*Corresponding author: bordas@ovgu.de

Two-phase wind tunnel

The existing Göttingen-type two-phase wind tunnel at the University of Magdeburg has been used with a closed test section (cross-section of 500×600 mm) for the experimental measurements described here. The optically accessible measurement section of the wind tunnel is 360×450×400 mm large. The velocity of the air flow has been varied between 3 and 25 m/s by prescribing a constant rotation speed of the fan, with the help of the frequency regulator of the wind tunnel. Water droplets have been generated with the help of an injection system upstream of the test section ($x = -620$ mm, with $x = 0$ at the entrance of the test section) using different water volume flow rates and various exchangeable spray heads. The turbulence intensity of the air flow has been measured to be around 10 %, for all configurations, since the spray head and the injection of the water droplets generate relatively high velocity fluctuations upstream of the test section. The relative humidity has been kept constant at saturation level during all measurements. The local flow conditions have been characterized by combinations of non-intrusive optical measurement methods in a previous project. Results of these measurements have been stored in an online data base (`www.ovgu.de/isut/lss/metstroem`), from which the required values can be retrieved and used when needed for the calculation of both theoretical and experimental collision rates.

Measurement configurations

Two different measurement cases have been considered, Case 1 being associated to large droplets (mean diameter around 400 μm) and Case 2 to small droplets (mean diameter around 10 μm). Case 1 is typically relevant for rain impact at ground level, while Case 2 corresponds to conditions encountered within cumulus clouds. The spray has been generated in Case 1 by a flat cone pressure atomizer (type CJM from Delavan) with a water volume flow rate of 5 l/min and a gauge pressure of 0.3 bar. For Case 2 a twin-fluid full cone pneumatic atomizing nozzle was employed with 60° cone angle (166.208.16.12 from the Co. Lechler), applying an air gauge pressure of 1.2 bar and a water volume flow rate of 0.1 l/min. To keep the inlet values constant, a PID-controller was programmed as well, in order to set the pump rotation speed according to the required volume flow rates. In this manner it is possible to create a steady water volume flow rate, leading to constant droplet mean diameters during the whole acquisition time, quite long indeed. In Case 1, a three-peak distribution has been obtained (peaks at 100 μm, 1 150 μm and 2 100 μm) leading to a mean droplet size of 400 μm, with droplet diameters up to 2 200 μm. On the other hand, the obtained droplet size distribution can be described in Case 2 by a probability density function as a two-parameter log-normal distribution (see also figure 1):

$$y = f(d|\mu,\sigma) = \frac{1}{d\sigma\sqrt{2\pi}} \exp\left[-\frac{(\ln(d)-\mu)^2}{2\sigma^2}\right], \tag{1}$$

with the shape and scale parameters $\sigma = 0.72$ and $\mu = 2.41$ respectively, i.e., the mean and standard deviation of the normal distribution. Using these parameters, the mean diameter (14.43 μm) and the standard deviation (11.89 μm) of the reconstructed log-normal distribution can be calculated as described in [3].

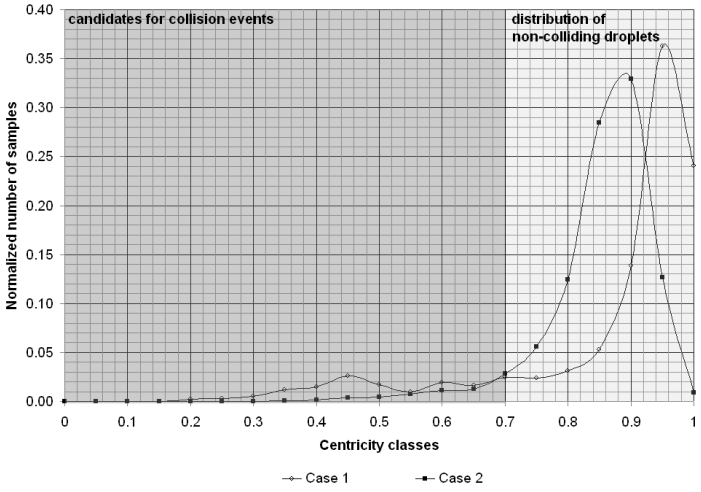

Figure 2. Probability density function of the centricity values.

Shadowgraphy

Shadowgraphy, applied here for the investigation of the droplet-droplet interactions is an imaging measurement method, relying typically on a CCD-camera, a far-field microscope, and a background illumination. For larger droplets, the velocity values should be determine as well. Therefore, a double-frame camera has been employed. The camera is an Imager Intense camera with a 2/3" CCD-sensor from LaVision (resolution: 1376×1040 pixel; pixel size: 6.45×6.45 μm) mounted with a Questar QM1 far-field microscope. The illumination has been provided by a double pulsed Nd:YAG laser (Litron) with a pulse energy of 300 mJ at a wavelength of 532 nm. With the help of the pulsed laser beams a fluorescence disc has been excited to get a homogeneous and powerful background illumination. A high intensity is required especially for the case of small droplets and corresponding small measurement volumes (Case 2). The camera and the illumination all lie on the same optical axis. As the droplets have been illuminated from behind, their shadow image has been recorded by the camera and the diameter of the droplets could be obtained with the help of a previously calibrated μm/pixel value [4, 5]. Since the expected collision rate is usually moderate in dispersed flows, and considering that the recording frequency of the applied camera is limited to 10 Hz, measurements leading to meaningful statistics must be carried out for a long period of time at a given position. The standard post-processing of the recorded images has been conducted using the commercial Shadowgraphy software DaVis 7.2 (LaVision). Following settings have been used during the batch processing:

Table 1. Batch processing settings in DaVis

1. **Intensity correction**			
Mean value	3000	counts	Mean intensity was corrected to this value
Threshold for droplets	1700	counts	If no values below this threshold, the image is skipped
2. **Set above/below constant**			
Lower level	2000	counts	Values below this level were set to this threshold
Upper level	3000	counts	Values above this level were set to this threshold
3. **Particle recognition**			
Global threshold	30	%	Intensity threshold for the 1st particle segmentation
Low level threshold	30	%	Threshold for low level diameters
High level threshold	50	%	Threshold for high level diameters
AOI expansion	50	%	Standard setting for the Area of Interest

Identification of collision events

The evaluation process follows a specific algorithm, which starts with the user-specific definition of a threshold value (see Table 1) and the automatic segmentation of the shadow regions on every image. Subsequently, the dimensions of the shadow regions are measured, in particular the smallest and largest axis length values as well as the segmented shadow area. From these quantities a diameter equivalent to the segmented area and the centricity (ratio of minimum to maximum axis) are obtained. The latter one is of central interest to further process and quantify collision events.

The collision events have been identified automatically in this way by batch post-processing of a considerable quantity of single images (typically $10\,000$). In order to get finally the collision probability, the resulting number of collision events has been divided by the total number of evaluated droplets during post-processing.

In order to identify collision events, the main idea is to use the centricity of the observed particles, as defined previously. The deformation of the droplets due to aerodynamic forces can be calculated theoretically as function of the dimensionless Weber number. Considering a linear correlation between the Weber number value and the

degree of aerodynamic droplet deformation [8], a correction of the centricity values has been carried out. The correction factor accounts for increased droplet deformation due to oscillations for higher droplet diameters and therefore allows lower centricity values to be accepted as valid for corresponding conditions. If the centricity falls outside of the tolerance range, this is an indication of a collision event.

If the droplets are small (Case 2) the Weber number is small as well and there is no significant droplet deformation. As a consequence, the correction procedure described previously is without effect. Nevertheless, the axis ratio should again be theoretically very close to 1.0. However, the measured values for centricity return a normal distribution between values of 0.7 and 1.0 (Figure 2) for both cases. This is due to slightly deformed droplets and even more to measurement uncertainties, in particular associated with the finite pixel resolution. The error induced by discretizing the true droplet boundaries on the pixels and thresholding is particularly important for the smallest droplets (Case 2).

The probability distribution of the centricity (built using $10\,000$ images with 0.6 droplet per image in average) is presented in Figure 2 for both cases. In the density distribution function two peaks can be recognized, for droplets with and without collision.

The upper limit for the identification of collision events should be set according to the distribution obtained for non-colliding droplets. In the present case, the corresponding threshold has been set to 0.7, as is depicted in Figure 2. As a result of this automatic batch processing, a list of Shadowgraphy images containing promising candidates for collision events is produced. In order to avoid artifacts and maximize accuracy, these candidate images are examined manually to exclude unsure events. Typical unsure collision events are exemplified in Figure 3. It is difficult to develop reliable automatic procedures to take care of those. Most of these unsure events are associated with particle(s) not in focus or to two droplets partly hiding each other in the depth of the image. Nevertheless, let us stress that the automatic batch processing is a very efficient and absolutely necessary help to analyze collision events. Typically, less than 50 images must be manually analyzed from $10\,000$ recorded images. Some exemplary collision events are presented in Fig. 4 for both small and large droplets (images at different scales).

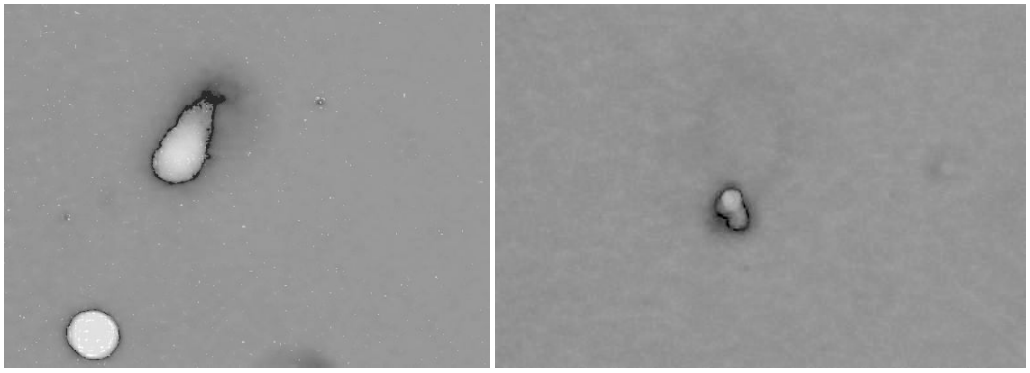

Figure 3. Examples for unsure collision events.

Results and Discussion

The employed evaluation algorithm, as described previously, is based on droplet shape recognition and discriminates collision events from aerodynamic droplet deformation, which is an essential issue when considering large droplet diameters. Therefore, it is now possible to employ the flat cone pressure atomizer and to test the developed experimental method for large droplets (Case 1). A theoretical prediction of collision probability can be found in the literature for corresponding conditions [6], where the collision rate is given as:

$$N = n^2 d^2 \left(\frac{4\pi \overline{u'^2}}{3} \right)^{1/2}, \tag{2}$$

yielding a collision probability of 0.007% for the present conditions. The quantities appearing in this equation are N, the number of collisions per unit volume and unit time, n the number of droplets per unit volume, with a diameter d and the RMS droplet velocities in the mean flow direction, u'. It should nevertheless be kept in mind that this equation is valid for single droplet size and not for a broad droplet size distribution, as in the present case.

After post-processing the experimental results of Shadowgraphy for Case 1, a local collision probability of

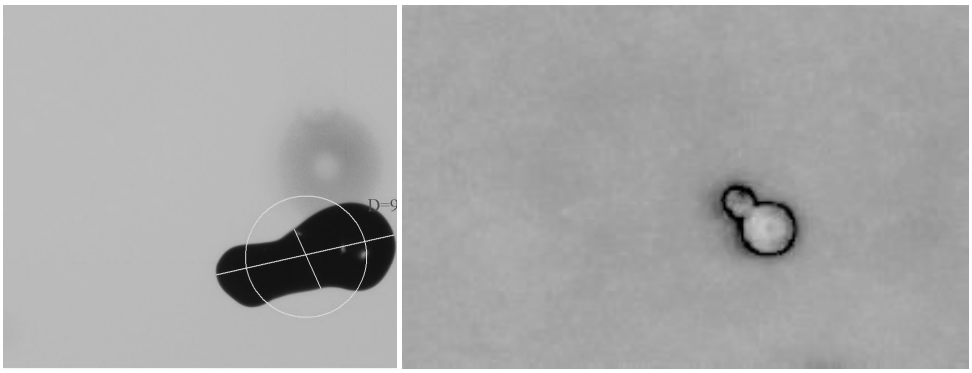

Figure 4. Example of a single collision event for Case 1 (left) and Case 2 (right).

0.439% has been measured in the center of the spray cone. In order to take into account the aerodynamic deformation of the droplets, the Weber number of every identified droplet has been first calculated; then, the expected centricity value has been modified according to the theoretical range of droplet deformation [9].

For Case 2, another theoretical model has been considered, suitable for the corresponding typical droplet size [7]:

$$N = n^2 d^2 (8\pi\overline{u'^2})^{1/2}, \tag{3}$$

with the same variables as in Eq. 2. Both models are based on the same theoretical considerations, however they deviate in a factor that results from the influence of gravity. Gravity has a more pronounced effect for large droplets and is only implicitly included within Eq. 2 after the simplification considering mono-disperse droplets.

Equation 3 gives a collision probability of 0.024 % for the present conditions. The experimentally measured collision probability using Shadowgraphy delivers a value of 0.053 %. Further parameters required to determine the collision probability for both equations have been obtained by complementary measurements based on Phase-Doppler Anemometry (PDA, for n and d) as well as Laser-Doppler Anemometry (LDA, for u').

In Table 2, the experimental collision rate has been calculated in two different manners, using either the data rate D or the concentration C respectively, both obtained from previous PDA measurements. The two results show the same order of magnitude. However, since previous works have shown that the PDA-based estimation of droplet concentration C is less reliable, the calculation based on the particle data rate D (divided by the PDA measurement volume) should probably be preferred.

Finally, the comparison between theoretical predictions and measured results shows qualitatively a good agreement for Case 2, where both values differ only by a factor 2. This slight increase is supported by the findings of other groups, for instance the observations discussed in [10]. A factor of 2 or more has been found between the predicted and the observed growth time for similar droplet sizes as in Case 2, which is assumed in [10] to be the result of a considerably underestimated theoretical prediction of collision probabilities.

On the other hand, the experimental result in Case 1 is much larger than the theoretical prediction (Table 2), with a factor 60 between both values. This is probably due to the single diameter value appearing in the theoretical calculation. For the multimodal size distribution of Case 1 (see again Fig. 1), the characterization of the distribution by a single, mean diameter does not make much sense. Furthermore, this value does not correspond to any of the 3 peaks observed in the distribution. Hence, the observed differences might be explained by the fact that both theoretical estimations considered here assume only a single value for mean diameter, velocity fluctuation and number density values. More complex correlations are certainly necessary for multi-peak distributions, like in Case 1.

Conclusions

In this work, the optimization of the Shadowgraphy technique for the investigation of droplet-droplet interactions has been presented. Using the developed method the collision probability, i.e., the number of colliding droplets divided by the number of droplets in a unit volume can be measured experimentally. All flow parameters needed for comparisons with theoretical estimations have been determined by means of different optical measurement techniques. All obtained results are collected in an experimental data-base accessible online (`www.ovgu.de/isut/lss/metstroem`). After measuring all parameters it becomes possible to calculate the collision rate from the measured collision probabilities and to compare with theoretical predictions, both for

Table 2. Results for both cases

Variable	Case 1	Case 2
Mean droplet diameter [μm]	399	14.5
Number density [#/m^3]	8.810e+6	5.737e+9
Mean particle velocity [m/s]	20.92	1.68
Mean flow velocity [m/s]	23.41	1.80
RMS flow velocity [m/s]	1.53	0.32
RMS particle velocity [m/s]	3.01	0.31
Viscosity of air [m^2/s]	1.54e-05	
Measured collision probability [%]	**0.439**	**0.053**
Droplet rate, calculated from D (or C) [#/m^{3}s]	9.74e+11 (1.81e+12)	4.53e+13 (2.13e+13)
Experimental collision rate from D (or C) [#/m^{3}s]	4.28e+9 (7.94e+9)	2.40e+10 (1.13e+10)
Theoretical collision rate [#/m^{3}s]	7.61e+7	1.07e+10
Experimental/theoretical collision rate from D (or C) [-]	**63.20** (117.38)	**2.25** (1.06)

large and for small droplet sizes. The comparisons show that both experiment predict higher collision rates than the models. The agreement is good for small droplets with a log-normal distribution, but poor for large droplets with a multi-peak distribution. Differences might be partly explained by the existing distributions of all important parameters in the experiments. The present findings must of course be refined and confirmed by many more systematic comparisons for other conditions.

Acknowledgement

The present project is part of SPP1276 - MetStroem funded by the German Research Foundation (DFG). The help and support of Vladimir Bogatkin during the analysis of Shadowgraphy measurements is gratefully acknowledged.

References

[1] Dodin, Z., and Elperin, T., *Physics of Fluids*, 14(8): 2921-2924 (2002).
[2] Pinsky, M., Khain, A., and Krugliak H., *Journal of the Atmospheric Sciences* 65(2): 357-374 (2008).
[3] Balakrishnan, N., and Chen, W. W. S., *Handbook of Tables for Order Statistics from Lognormal Distributions with Applications*, Kluwer, 1999, p. 5.
[4] Bordás, R., Öncül, A.A., Zähringer, K., Thévenin, D., *12th International Symposium on Flow Visualization*, Göttigen, Germany, September 2006, pp. 14.1-14.10.
[5] Kapulla, R., Trautmann, M., Hernandez Sanchez, A., Calvo, Zaragoza, S., Hofstetter, S., Häfeli, C., and Güntay, S., *15. Fachtagung Lasermethoden in der Strömungsmesstechnik*, Rostock, Germany, September 2007, pp. 27.1-27.6.
[6] Abrahamson, J., *Chemical Engineering Science* 30(11): 1371-1379 (1975).
[7] Williams, J. J. E., and Crane, R. I., *International Journal of Multiphase Flow*, 9(4), 421-432 (1983).
[8] Pilch, M., and Erdman, C. A., *International Journal of Multiphase Flow*, 13(6), 741-757 (1987).
[9] Hsiang, L.P., and Faeth, G. M., *International Journal of Multiphase Flow*, 18(5), 635-652 (1992).
[10] Xue, Y., Wang, L. P. and W. W. Grabowski, *Journal of the Atmospheric Sciences*, 65(2), 331-356 (2008).